Amino Acids (2012) 42:775–781
DOI 10.1007/s00726-011-0994-z

ORIGINAL ARTICLE

Protective effects of agmatine in rotenone-induced damage of human SH-SY5Y neuroblastoma cells: Fourier transform infrared spectroscopy analysis in a model of Parkinson's disease

Salvatore Condello · Emanuele Calabrò · Daniela Caccamo · Monica Currò · Nadia Ferlazzo · Joseph Satriano · Salvatore Magazù · Riccardo Ientile

Received: 4 March 2011 / Accepted: 16 May 2011 / Published online: 31 July 2011

Abstract Agmatine is a novel neuromodulator that plays a protective role in the CNS in several models of cellular damage. However, the mechanisms involved in these protective effects in neurodegenerative diseases are poorly understood. Fourier transform infrared (FTIR) spectroscopy analysis detects biomolecular changes in disordered cells and tissues. In this report, we utilize FTIR spectroscopy to characterize the changes in rotenone-induced damage in neuronal-like differentiated SH-SY5Y neuroblastoma cells in the presence or absence of agmatine. The analysis of the FTIR spectra demonstrates significant alterations in rotenone-treated cells, whereas the FTIR spectra obtained after pre-incubation with agmatine (250 nM) significantly reduces these redox alterations and more closely resembles those of the control cells. In particular, rotenone-damaged cells demonstrate spectral alterations related to amide I, which correspond to an increase in β-sheet components, and decreases in the amide II absorption intensity, suggesting a loss of N–H bending and C–N stretching. These alterations were also evident by Fourier self-deconvolution analysis. Thus, rotenone-induced increases in the levels of stretching vibration band related to the protein carboxyl group would account for a significant amount of misfolded proteins in the cell. Agmatine effectively reduces these effects of rotenone on protein structure. In conclusion, antioxidant and scavenging properties of agmatine reduce rotenone-produced cellular damage at the level of protein structure. These, together with other previous observations, demonstrate the therapeutic potential of agmatine in the treatment of Parkinson's disease.

Keywords Agmatine · Fourier transform infrared spectroscopy · SH-SY5Y neuroblastoma cells · Reactive oxygen species · Membrane mitochondrial potential · Neuroprotection

Abbreviations

FTIR	Fourier transform infrared
NF-κB	Nuclear factor κB
PD	Parkinson's disease
ROS	Reactive oxygen species
$\Delta\psi_m$	Mitochondrial membrane potential
Rh-123	Rhodamine-123
FSD	Fourier self-deconvolution
ATR	Attenuated total reflection; asymmetric stretching vibration
$^{as}COO^-$	Unprotonated carboxyl group
$^{s}COO^-$	Symmetric unprotonated carboxyl group

Introduction

Rotenone-induced cell damage in neuronal-like dopaminergic cells is associated with reduced activity of mitochondrial complex I resembling neurodegenerative

S. Condello · D. Caccamo · M. Currò · N. Ferlazzo · R. Ientile (✉)
Department of Biochemical, Physiological and Nutritional Sciences, Policlinico Universitario "G. Martino", Via C. Valeria, 98125 Messina, Italy
e-mail: ientile@unime.it

E. Calabrò · S. Magazù
Department of Physics, University of Messina, Messina, Italy

J. Satriano
Department of Medicine, University of California, San Diego, and Veterans Administration San Diego Healthcare System, La Jolla, CA, USA

mechanisms observed in Parkinson' disease (PD) (Mizuno et al. 1989; Xie et al. 2010). Mitochondrial dysfunction has been proposed as a principal component in the pathogenesis of PD (Ben-Shachar et al. 1991; Schapira 2006). Evidence from animal models suggests that rotenone induces oxidative effects that are responsible for some of the toxicity, and that these effects can be blocked by antioxidant therapy (Kim et al. 2008; Clark et al. 2010). However, there currently remain no known treatments to suppress the progression of neuronal cell injury and death, with clinical intervention limited primarily to palliative care (Morley and Hurtig 2010; Kang et al. 2010).

Recently, we reported that exposure to agmatine, the endogenous metabolite of arginine, demonstrates protective effects in the rotenone model of cell injury in human-derived dopaminergic neuroblastoma cell line (SH-SY5Y) (Condello et al. 2011). The neuroprotective action of agmatine was associated with suppression of rotenone induction of nuclear factor-κB (NF-κB) nuclear translocation, reactive oxygen species (ROS), mitochondrial membrane dissipation, and the apoptotic-signaling cascade. Our results are in accordance with findings indicating that agmatine may cause attenuation of cell damage resulting from reactive oxygen production, and hypoxia-induced alterations (Hong et al. 2007; Iizuka et al. 2008; Agostinelli et al. 2010; Ahn et al. 2011), and is able to reduce oxidative damage by scavenger effects or inhibiting receptor-mediated alterations (Roberts et al. 2005; Gilad et al. 2005; Battaglia et al. 2010). Furthermore, we recently reported that protective effects of agmatine are associated with suppression of apoptosis through stabilization of mitochondrial function (Arndt et al. 2009).

Several different and complementary experimental techniques have been employed in the study of biological systems as potential tools to provide, in near real time, information about the different biochemical and morphological structures in normal and altered conditions. Fourier transform infrared (FTIR) spectroscopy is a method of vibration spectroscopy, extremely sensitive to molecular structural changes (Zhang et al. 2007; Di Giambattista et al. 2010). In particular, this technique provides information concerning the structure and interactions of, but not limited to, proteins, lipids, and nucleic acids, both in isolation and in complex assemblies. These features provide biochemical information at the onset of the disease, prior to the morphological manifestations or downstream complications of the disease itself.

Previously, we demonstrated that agmatine administration preserves mitochondrial membrane potential ($\Delta\psi_m$) thereby counteracting rotenone-induced cell damage in neuronal-like differentiated SH-SY5Y neuroblastoma cells. Herein, we present FTIR spectroscopy data related to biochemical and structural changes resulting from rotenone-induced cell stress, and the protective effects of agmatine in this model of PD.

Materials and methods

The human neuroblastoma SH-SY5Y cell line (CRL-2266) was purchased from American Type Culture Collections (ATCC) (Rockville, Maryland, USA). Eagle's minimum essential medium, Ham's F-12 nutrient mixture, fetal bovine serum (FBS), penicillin/streptomycin mixture, *all-trans* retinoic acid (RA), 3-(4, 5-methylthiazol-2-yl)-2, 5-diphenyl-tetrazolium bromide (MTT), 2′,7′-dichlorofluorescein diacetate (H2DCF-DA), dimethylsulfoxide (DMSO), glutamine, sodium pyruvate, phosphate buffered saline solution (PBS), other chemicals of analytical grade, were from Sigma (Milan, Italy).

Cell culture and treatment

Human neuroblastoma SH-SY5Y cells were maintained at 37°C in a humidified incubator with 5% CO_2 and 95% air, and cultured in MEM/Ham's F12 (1:1) medium containing 10% (v/v) FBS, L-glutamine (2 mM), sodium pyruvate (1 mM), and 10 U/ml penicillin, and 100 mg/ml streptomycin. Sub-confluent cells were washed twice with PBS, then incubated in MEM/Ham's F12 medium containing 10 μM retinoic acid (10 mM in DMSO stock solution), 1% FBS, L-glutamine (2 mM), sodium pyruvate (1 mM). The medium was renewed every 2 days. After 5 days of 10 μM retinoic acid (RA) exposure, differentiated SH-SY5Y cells were incubated with rotenone (500 nM) for 24 h in the presence or absence of agmatine (250 nM) which were added to the culture medium 30 min prior to rotenone treatment.

Evaluation of cell viability and ROS production

Cell viability was evaluated by an MTT quantitative colorimetric assay as previously reported (Condello et al. 2011). ROS was quantified using the non-fluorescent probe 2′-7′-dichlorofluorescein (DCF) diacetate, which could be oxidized to highly fluorescent compound DCF upon exposure to ROS, as previously described (Condello et al. 2011).

Measurement of $\Delta\psi_m$

Changes in $\Delta\psi_m$ were assayed by the incorporation of a cationic fluorescent dye rhodamine-123 (Rh-123). After treatments as previously described, the cells (2.5×10^5 cells/ml in 6-well plates) were changed to fresh medium containing 10 μM Rh-123 and incubated for 15 min at

37°C. The cells were then collected, washed twice with PBS (pH 7.4) and the fluorescence intensity was analyzed at wavelength of 488-nm excitation and 525-nm emission by a microplate reader (Tecan Italia, Cologno Monzese, Italy).

Infrared spectroscopy

Fourier transform infrared spectroscopy data were obtained in rotenone-treated cultures in the presence or absence of agmatine (250 nM). After rotenone treatment RA-differentiated SH-SY5Y cells (5×10^5 cells/ml in 25 cm^2 culture flask) were washed twice with PBS (pH 7.4), harvested with non-enzymatic cell dissociation solution (Sigma (Milan, Italy), centrifuged at 800 rpm for 10 min and re-suspended in 50 µl of PBS. This volume was transferred to a slide and air-dried.

Then, cells were placed upon the CaF_2 windows for FTIR measurements. FTIR spectra were recorded by a Bruker Optics, Vertex 80v spectrometer.

The attenuated total reflection technique was chosen for spectrum collection, as it allows overcoming solvent masking. The penetration depth of infrared light is inherently limited to a fraction of the wavelength of about $\lambda/10$ (Smith and Franzen 2002) allowing secondary structure analyses on small volumes. For each spectrum, 64 interferograms were collected with a spectral resolution of 4 cm^{-1} in the range from 4,000 to 1,000 cm^{-1}. The infrared spectra were baseline-corrected and area-normalized for treated and control samples, as accurately described in Calabrò and Magazù (2010).

In addition, Fourier self-deconvolution (FSD) allows identifying the peak frequencies of the characteristic spectral components providing a more detailed qualitative assessment. FSD was applied to enhance vibration features of spectra to our samples using the following parameters: Lorentzian shape with bandwidth = 16.33, deconvolution factor = 3, and noise reduction factor = 0.5.

Statistical analysis

All values are expressed as mean ± SEM Statistical analysis was carried out using Student's *t* test for comparisons between two groups with $p < 0.05$ considered significant.

Results

Human neuroblastoma SH-SY5Y cells can be differentiated in vitro to a neuronal phenotype by RA treatment. We observed that extension of neurites, a typical neuronal phenotype, was present 5 days after application of RA while undifferentiated cells maintained relatively short neurites. Cell differentiation was also checked by the expression of α-tubulin, as neuron specific marker (resulting in the about fivefold increase vs. untreated cells).

We first evaluated the effects of rotenone on cellular redox state. Rotenone incubation produced redox alterations leading to a significant increase in relative DCF fluorescence, representative of ROS levels. Agmatine administration dose-dependently decreased this rotenone-induced ROS production with the highest concentration (250 nM) restoring the cells to control levels (Fig. 1). This concentration of agmatine was utilized in the remaining experiments evaluating the protective effects from rotenone toxicity.

Cell damage was evaluated by MTT assay. Rotenone diminished MTT reduction up to 58 ± 5.5% of control level. Under these conditions, agmatine administration suppressed rotenone effects on cell viability and the degree of MTT reduction was about 80 ± 4.8% of controls (Fig. 2a). Considering that rotenone-induced ROS production is a major contributor to rotenone toxicity and cell death, and that ROS is causal to the dissipation of $\Delta\psi_m$, we examined if this effect is also counteracted by agmatine administration. In comparison to controls, rotenone exposure significantly decreased Rh-123 fluorescence, a probe for measurement of $\Delta\psi_m$, by approximately 40 ± 2.5%. Cell cultures pre-treated with agmatine before rotenone administration protected the cells from this decline in fluorescence and again approached control, non-rotenone

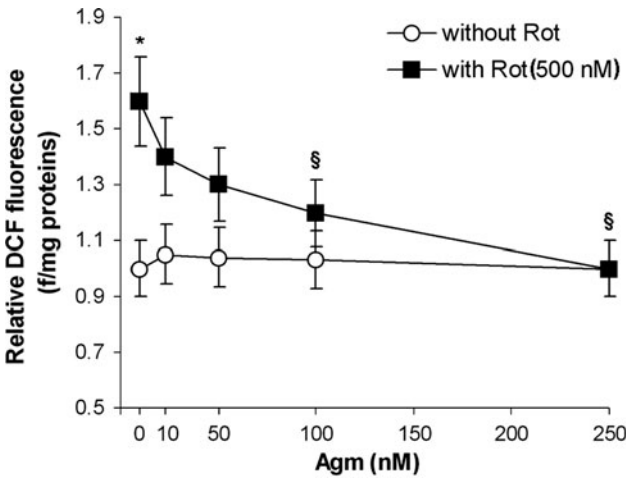

Fig. 1 Effects of agmatine on rotenone-induced ROS production in RA-differentiated SH-SY5Y cells. Cell cultures were incubated with rotenone (*Rot* 500 nM) for 24 h in the presence or absence of agmatine (*Agm*) at indicated concentrations which was added to the culture medium 30 min prior to rotenone treatment. Intracellular ROS production was determined by DCF fluorescence as reported in "Materials and methods". The results are expressed as fold increase of the fluorescence intensity over untreated control cells. Data from 5–6 experiments are expressed as mean ± SEM. Significant differences: $^*p < 0.05$ versus control, $^§p < 0.05$ versus rotenone

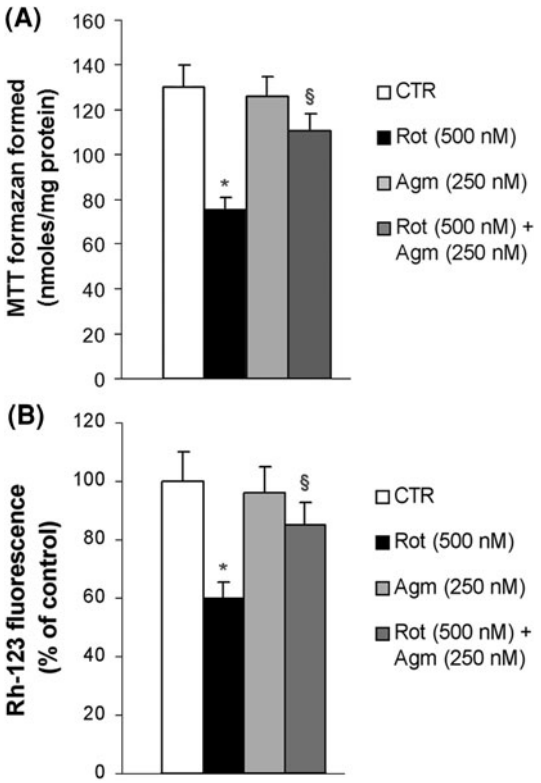

Fig. 2 Protective effects of agmatine against rotenone-induced cell damage. **a** Effects of agmatine on rotenone-induced cytotoxicity in SH-SY5Y cells. Cell cultures were incubated with rotenone (*Rot*) for 24 h in the absence or presence of agmatine (*Agm* 250 nM) as per Fig. 1. Cell viability was assayed using the MTT method. Values are expressed as the percentage of the untreated control and represented as mean ± SEM of at least five independent experiments. Significant differences: $^{*}p < 0.05$ versus control, $^{\S}p < 0.05$ versus rotenone treatment, respectively. **b** Effects of agmatine on rotenone-induced $\Delta\psi_m$ loss in RA-differentiated SH-SY5Y cells. Cell cultures were incubated with rotenone for 24 h in the presence or absence of agmatine (250 nM) which was added to the culture medium 30 min prior to rotenone treatment, as per Fig. 1. Changes in $\Delta\psi_m$ were assessed using cationic dye Rh-123. Cells were collected from culture plates and rhodamine-123 fluorescence was measured by fluorimetry. Mean ± SEM from six experiments are expressed as percentage of controls. Significant differences: $^{*}p < 0.05$ versus control, $^{\S}p < 0.05$ versus rotenone group, respectively

levels. This data confirms earlier work that agmatine protects mitochondrial function from rotenone injury (Fig. 2b).

The bioprotective effectiveness of agmatine was also investigated by means of FTIR spectroscopy in mid-infrared region. Preliminary data demonstrated that agmatine added alone produced an FTIR spectrum superimposable with control (data not shown). FTIR analysis evidenced an upshift from 1,651 to 1,657 cm^{-1} in the centroid of the amide I band peak occurring after the treatment with rotenone (500 nM) (Fig. 3a). In addition, rotenone induced an evident decrease in the amide II absorption intensity as well (around 1,538 cm^{-1}) suggesting a loss of N–H bending and C–N stretching. Preliminary addition of agmatine counteracts both these effects (Fig. 3a). Changes in attenuated total reflection (ATR) units were also evaluated in the ranges 1,595–1,560 and 1,430–1,390 cm^{-1}. Rotenone significantly increased the vibration bands intensities relative to these frequency values, whereas the preliminary addition of agmatine yielded no appreciable alterations and ATR units reached the control values. These bands may be assigned to asymmetric unprotonated carboxyl group ($^{as}COO^{-}$) and symmetric unprotonated carboxyl group ($^{s}COO^{-}$) stretching vibration modes, respectively (Barth 2000; Fabian and Vogel 2002).

To emphasize the spectral structure, FSD analysis was applied to the acquired spectra. The upshift of the amide I peak centroid corresponding to cells treated with rotenone was enhanced in comparison to the control (Fig. 3b). A relative increase in the β-sheet contents at 1,635 and 1,685 cm^{-1} with respect to the α-helix component was also evident in the amide I mode, whereas no increase in β-sheet components was detectable in the cell samples cultured in the presence of agmatine.

The increase in both vibration bands of the unprotonated carboxyl groups after treatment with rotenone was enhanced by FSD analysis as well. Furthermore, changes were also observed in the frequency bands of CH_2 bending modes, as downshifts from 1,464 to 1,454 cm^{-1} and from 1,350 to 1,343 cm^{-1} occurring the spectra from cell cultures after the addition of rotenone. Apparently, the addition of agmatine was not able to counteract these effects (Fig. 3b).

Quantitative results were also obtained from the acquired spectra by the integrated area from 1,590 to 1,570 cm^{-1} and from 1,420 to 1,390 cm^{-1} corresponding to $^{as}COO^{-}$ and $^{s}COO^{-}$ stretching vibration band of carboxyl group, respectively. Statistical analysis demonstrated that in comparison to controls the integrated area corresponding to $^{as}COO^{-}$ and $^{s}COO^{-}$ the spectra of cell cultures in the presence of rotenone significantly increased in comparison to controls ($p < 0.0001$ and 0.001, respectively), whereas no appreciable changes were observed in the presence of agmatine (Fig. 4a, b). Furthermore, the band around 1,515 cm^{-1}, due to tyrosine, was observed in the spectra of samples in the presence of rotenone. Because changes in the tyrosine band absorbance occur when hydrophobic cores of a protein are formed, this spectral shift has been considered a specific local marker for protein conformational change (Fabian et al. 1993).

Discussion

Various studies have been reported supporting the neuroprotective effects of agmatine, including our recent report in the rotenone toxicity in SH-SY5Y neuroblastoma cell

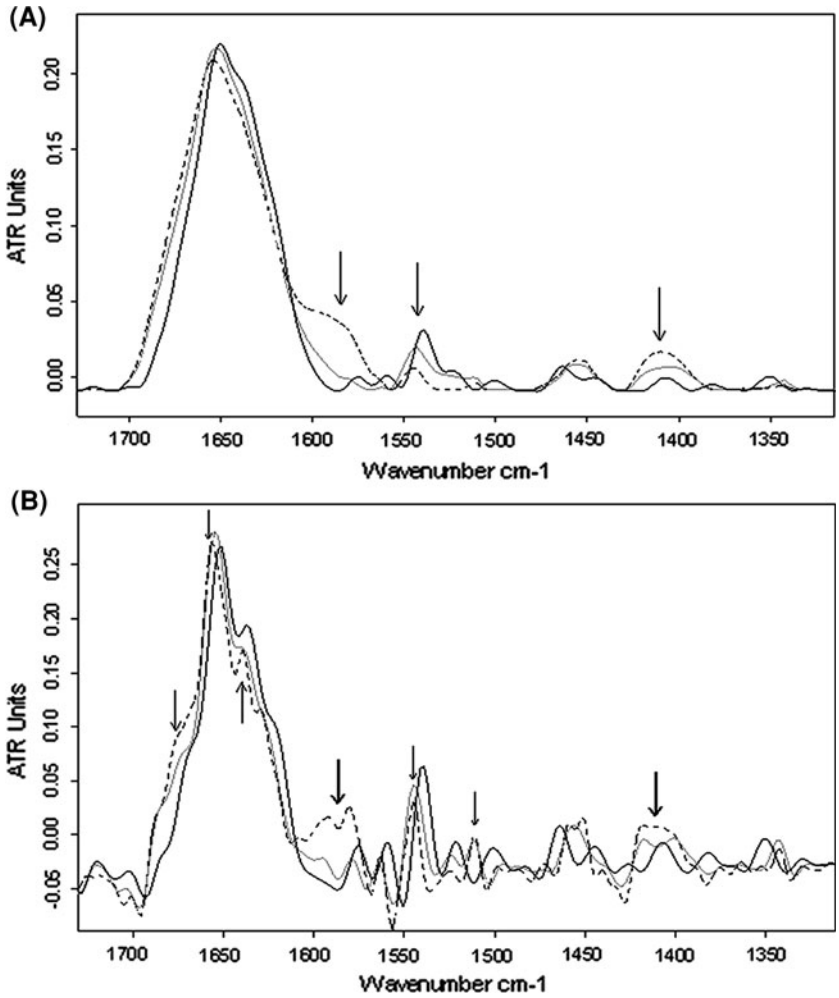

Fig. 3 **a** Typical ATR spectra in the amides I, II and III regions, for SH-SY5Y neuroblastoma cells samples (*solid thin line*). Cells were incubated with rotenone (500 nM), for 24 h in the absence (*thick solid line*) or in the presence of agmatine (250 nM) (*dotted line*), respectively. Agmatine alone did not change FTIR spectrum in comparison to controls, whereas an upshift from 1,651 to 1,657 cm^{-1} of the amide I band peak centroid can be observed after treatment with rotenone. The regions in the ranges 1,595–1,560 cm^{-1} and 1,430–1,390 cm^{-1} (both indicated by *arrows*) appeared to increase significantly in the presence of rotenone, whereas no appreciable changes occurred in the presence of agmatine. **b** Fourier self-deconvolution analysis applied to the same spectra of section A. An increase in the β-sheet contents at 1,635 and 1,685 cm^{-1} appeared also in the amide I region with rotenone, but not when in the presence of agmatine

model of PD (Gilad et al. 2005; Arndt et al. 2009; Condello et al. 2011). Here, we first confirmed the formation of radicals in neuronal-like differentiated cells exposed to rotenone. Although it seems reasonable that exogenous antioxidants could be utilized in diminishing the cumulative effects of oxidative stress, antioxidant therapy has not yet proven a proficient course of treatment in the clinic. Agmatine also demonstrates antioxidant cell protection with free-radical scavenging properties, and here we verify its capacity to protect against rotenone-induced alterations in the cellular redox state. The current study was carried out specifically to further evaluate the relationship between changes in the protein structures and redox status associated with the protective effects of agmatine.

Indeed, the results from the FTIR spectroscopy uncover information about the protein secondary structures in this model. The amides I and II bands observed at approximately 1,650 and 1,550 cm^{-1} in the FTIR spectra, respectively, are of particular interest. The band viewed at about 1,650 cm^{-1} is defined as amide I band and arises from the amide C=O stretching vibration and N–H bending mode (Surewicz and Mantsch 1988). Under our conditions, it appears that rotenone-induced changes in the amide I band are derived from alterations of the β-sheet of proteins (Ismail et al. 1992; Lefevre and Subirade 2000). However, a relative increase in β-turn content (around 1,660 cm^{-1}) with respect to α-helix component in the protein secondary structure may occur as well. When considering the observed spectral changes in the presence of agmatine, it is possible to hypothesize that these effects can be due to the interaction of a polycation structure of this compound with C=O and C–N groups of proteins. The addition of agmatine to rotenone-treated cells produced differences in spectra exhibiting positive changes at 1,657 cm^{-1} for the amide I and at 1,545 cm^{-1} for the amide II bands, as indicative of major cation–protein interactions which are associated with protective effects on protein structure. β-turns are associated with characteristic bands from 1,663 to 1,690 cm^{-1} (Jackson and Mantsch 1995; Kong and Yu 2007). With rotenone, the typical ATR spectra showed a relative increase near 1,660 cm^{-1} of β-turn content, with respect to the α-helix component in the protein secondary structure that may have occurred as well.

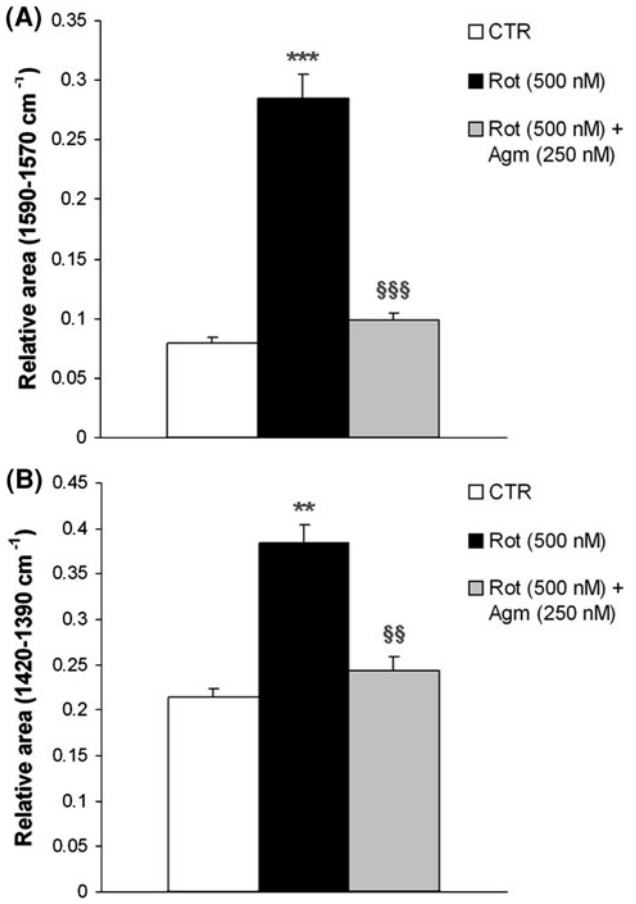

Fig. 4 Rotenone effects in stretching vibration bands of the unprotonated carboxyl group. **a** The *histogram* represents the integrated area computed from 1,590 to 1,570 cm^{-1} relative to the asymmetric stretching vibration band^{asCOO-}, and **b** the integrated area computed from 1,420 to 1,390 cm^{-1} relative to the symmetric stretching vibration bands $^{s}COO^{-}$ for SH-SY5Y neuroblastoma cells samples in the presence of rotenone, and in the presence of rotenone and agmatine. The data represent the mean ± SEM from six experiments. Significant differences $^{**}p < 0.001$, $^{***}p < 0.0001$ in comparison to control group, $^{§§}p < 0.001$, $^{§§§}p < 0.0001$ in comparison to rotenone-treated cultures

Several lines of evidence indicate that misfolded proteins, such as tubulin, may be involved in PD (Galloway et al. 1992). In addition to its widely recognized ability to inhibit mitochondrial complex I, rotenone also potently depolymerizes microtubules in vivo and in vitro (Higgins and Greenamyre 1996; Marshall and Himes 1978). This degradation of tubulin in response to neurotoxins is involved in PD (Ren et al. 2003). More so, the inhibition of complex I by rotenone leads to overproduction of ROS, which covalently modify many cellular proteins and increases their misfolding. A combination of the two activities of this toxin would produce a significant accumulation of misfolded proteins in the cell, which could become toxic (Giasson and Lee 2001).

A question that arises from these results is whether there is any connection with the neurodegenerative mechanisms shown in PD. Many of the disease complications in PD are well accounted for by the relationship between oxidative conditions and altered protein folding (Cuervo et al. 2010). Here, we demonstrate that antioxidant effects of agmatine in the model of rotenone-induced neuronal damage may be related to the observed reduction of β-sheet components (Ismail et al. 1992; Lefevre and Subirade 2000). A more detailed investigation would be needed to explore the underlying mechanisms.

The antioxidant properties of natural compounds are of great interest due to the potential of replacing synthetic antioxidants with natural ones that may reinstate components of a natural protective response and provide a more effective therapy. Our results indicate that agmatine has the capacity to scavenge free radicals and that this can protect cells against apoptotic cell damage (Condello et al. 2011). The results from FTIR detailed analysis further show that agmatine administration counteracts rotenone-induced structural changes occurring in proteins as a function of its folded/unfolded state transition. This preliminary report will also provide the basis for further studies in this area in the hopes of future clinical application.

References

Agostinelli E, Marques MP, Calheiros R, Gil FP, Tempera G, Viceconte N, Battaglia V, Grancara S, Toninello A (2010) Polyamines: fundamental characters in chemistry and biology. Amino Acids 38:393–403

Ahn SK, Hong S, Park YM, Lee WT, Park KA, Lee JE (2011) Effects of agmatine on hypoxic microglia and activity of nitric oxide synthase. Brain Res 1373:48–54

Arndt MA, Battaglia V, Parisi E et al (2009) The arginine metabolite agmatine protects mitochondrial function and confers resistance to cellular apoptosis. Am J Physiol Cell Physiol 296:C1411–C1419

Barth A (2000) The infrared absorption of amino acid side chains. Prog Biophys Mol Biol 74:141–173

Battaglia V, Grancara S, Satriano J, Saccoccio S, Agostinelli E, Toninello A (2010) Agmatine prevents the $Ca^{(2+)}$-dependent induction of permeability transition in rat brain mitochondria. Amino Acids 38:431–437

Ben-Shachar D, Riederer P, Youdim MB (1991) Iron-melanin interaction and lipid peroxidation: implications for Parkinson's disease. J Neurochem 57:1609–1614

Calabrò E, Magazù S (2010) Inspections of mobile phone microwaves effects on proteins secondary structure by means of Fourier transform infrared spectroscopy. J Electromag Anal Appl 2:607–617

Clark J, Clore EL, Zheng K, Adame A, Masliah E, Simon DK (2010) Oral *N*-acetyl-cysteine attenuates loss of dopaminergic terminals in alpha-synuclein overexpressing mice. PLoS One 5(8):e12333

Condello S, Currò M, Ferlazzo N, Caccamo D, Satriano J, Ientile R (2011) Agmatine effects on mitochondrial membrane potential and NF-κB activation protect against rotenone-induced cell

damage in human neuronal-like SH-SY5Y cells. J Neurochem 116:67–75

Cuervo AM, Wong ES, Martinez-Vicente M (2010) Protein degradation, aggregation, and misfolding. Mov Disord 25:S49–S54

Di Giambattista L, Grimaldi P, Gaudenzi S, Pozzi D, Grandi M, Morrone S, Silvestri I, Congiu Castellano A (2010) UVB radiation induced effects on cells studied by FTIR spectroscopy. Eur Biophys J 39:929–934

Fabian H, Vogel HJ (2002) Fourier transform infrared spectroscopy of calcium-binding proteins. Methods Mol Biol 173:57–74

Fabian H, Schultz C, Naumann D, Landt O, Hahn U, Saenger WJ (1993) Secondary structure and temperature-induced unfolding and refolding of ribonuclease T1 in aqueous solution. Mol Biol 232:967–981

Galloway PG, Mulvihill P, Perry G (1992) Filaments of Lewy bodies contain insoluble cytoskeletal elements. Am J Pathol 140:809–822

Giasson BI, Lee VM (2001) Parkin and the molecular pathways of Parkinson's disease. Neuron 31:885–888

Gilad GM, Gilad VH, Finberg JP, Rabey JM (2005) Neurochemical evidence for agmatine modulation of 1-methyl-4-phenyl-1, 2, 3, 6-tetrahydropyridine (MPTP) neurotoxicity. Neurochem Res 30:713–719

Higgins DS, Greenamyre JT (1996) [H-3]dihydrorotenone binding to NADH: ubiquinone reductase (complex I) of the electron transport chain: an autoradiographic study. J Neurosci 16:3807–3816

Hong S, Lee JE, Kim CY, Seong GJ (2007) Agmatine protects retinal ganglion cells from hypoxia-induced apoptosis in transformed rat retinal ganglion cell line. BMC Neurosci 8:81

Iizuka Y, Hong S, Kim CY, Kim SK, Seong GJ (2008) Agmatine pretreatment protects retinal ganglion cells (RGC-5 cell line) from oxidative stress in vitro. Biocell 32:245–250

Ismail AA, Mantch HH, Wong PTT (1992) Aggregation of chymotrypsinogen: portrait by infrared spectroscopy. Biochim Biophys Acta 1121:183–188

Jackson M, Mantsch HH (1995) The use and misuse of FTIR spectroscopy in the determination of protein structure. Crit Rev Biochem Mol Biol 30:95–120

Kang SY, Wasaka T, Shamim EA, Auh S, Ueki Y, Lopez GJ, Kida T, Jin SH, Dang N, Hallett M (2010) Characteristics of the sequence effect in Parkinson's disease. Mov Disord 25: 2148–2155

Kim HY, Chung JM, Chung K (2008) Increased production of mitochondrial superoxide in the spinal cord induces pain behaviors in mice: the effect of mitochondrial electron transport complex inhibitors. Neurosci Lett 447:87–91

Kong J, Yu S (2007) Fourier transform infrared spectroscopic analysis of protein secondary structures. Acta Biochim Biophys Sin 39:549–559

Lefevre T, Subirade M (2000) Molecular differences in the formation and structure of fine-stranded and particulate β-lactoglobulin gels. Biopolymers 54:578–586

Marshall LE, Himes RH (1978) Rotenone inhibition of tubulin self-assembly. Biochim Biophys Acta 543:590–594

Mizuno Y, Ohta S, Tanaka M, Takamiya S, Suzuki K, Sato T, Oya H, Ozawa T, Kagawa Y (1989) Deficiencies in complex I subunits of the respiratory chain in Parkinson's disease. Biochem Biophys Res Commun 163:1450–1455

Morley JF, Hurtig HI (2010) Current understanding and management of Parkinson disease: five new things. Neurology 75:S9–S15

Ren Y, Zhao J, Feng J (2003) Parkin binds to alpha/beta tubulin and increases their ubiquitination and degradation. J Neurosci 23:3316–3324

Roberts JC, Grocholski BM, Kitto KF, Fairbanks CA (2005) Pharmacodynamic and pharmacokinetic studies of agmatine after spinal administration in the mouse. J Pharmacol Exp Ther 314:1226–1233

Schapira AH (2006) Etiology of Parkinson's disease. Neurology 66:S10–S23

Smith BM, Franzen S (2002) Single-pass attenuated total reflection Fourier transform infrared spectroscopy for the analysis of proteins in H_2O. Sol Anal Chem 74:4076–4080

Surewicz WK, Mantsch HH (1988) New insight into protein secondary structure from resolution-enhanced infrared spectra. Biochim Biophys Acta 952:115–130

Xie HR, Hu LS, Li GY (2010) SH-SY5Y human neuroblastoma cell line: in vitro cell model of dopaminergic neurons in Parkinson's disease. Chin Med J (Engl) 123:1086–1092

Zhang G, Moore DJ, Flach CR, Mendelsohn R (2007) Vibrational microscopy and imaging of skin: from single cells to intact tissue. Anal Bioanal Chem 387:1591–1599